Gas-Ice Partitioning Coefficients of Carbonyls during Diffusional Ice Crystal Growth

Jackson Seymore*[1], Miklós Szakáll[1], Alexander Theis[3], Subir Mitra[3], Christine Borchers[2], Thorsten Hoffmann[2]

[1] Institute for Atmospheric Physics, Johannes Gutenberg University, Mainz, Germany
[2] Department of Chemistry, Johannes Gutenberg–University, Mainz, Germany
[3] Particle Chemistry Department, Max Planck Institute for Chemistry, Mainz, Germany

*Corresponding author: seymorej@uni-mainz.de

Table S1. Bubbler Concentrations and Henry Solubilities

	H^{cp}		**$H_s^{cp}T$**	**Target Flowtube Gas Concentration**	**Molar Mass**	**Target Bubbler Liquid concentration (uM)**		
	mol/(m^3 Pa)	M/atm	K	ppbv	g/mol	-40 ºC (d =165)	-30 ºC (d = 55)	-20 ºC (d = 18)
Benzaldehyde	0.4	40.53	5200	10	106.12	109	36	12
MVK	0.26	26.34	7800	10	70.09	91	30	10
Methacrolein	0.045	4.56	4600	10	70.09	12	4	1
Acetaldehyde	0.13	13.17	5900	10	44.05	38	13	4
Formaldehyde	32	3242.4	7100	10	30.03	10447	3482	1159
Acetone	0.27	27.36	5500	10	58.08	76	25	8
Nopinone	14	1418.55		10	138.21	2341	780	260
Norcamphor	0.43	43.57	5100	10	110.15	116	39	13
Camphor	0.54	54.72	4800	10	152.23	142	47	16
Diacetyl	0.73	73.97	5700	10	86.09	209	70	23
Glyoxal	4100	415433	7500	10	58.04	1389975	463325	154161
Hydroxyacetone	77	7802.03		10	74.08	12873	4291	1428
Methylglyoxal	35	3546.38	7500	10	72.06	11866	3955	1316
Propionaldehyde	0.099	10.03	4300	10	58.08	25	8	3

Table S2. Target m/z for MS analysis (Compounds given in elution order)

Species	Elemental Formula	Monoisotopic Mass (Da)	MS Analyte	Analyte Elemental Formula	Target m/z used $[M-H]^-$	Expected RT (min)
Hydroxyacetone	$C_3H_6O_2$	74.0368	Hydroxyacetone-DNPH	$C_9H_{10}N_4O_5$	253.0573	1.3
Formaldehyde	CH_2O	30.0106	Formaldehyde-DNPH	$C_7H_6N_4O_4$	209.0311	1.9
Acetaldehyde	C_2H_4O	44.0262	Acetaldehyde-DNPH	$C_8H_8N_4O_4$	223.0467	2.7
Acetone	C_3H_6O	58.0419	Acetone-DNPH	$C_9H_{10}N_4O_4$	237.0624	3.5
Propionaldehyde	C_3H_6O	58.0419	Propionaldehyde-DNPH	$C_9H_{10}N_4O_4$	237.0624	3.9
Methacrolein	C_4H_6O	70.0419	Methacrolein-DNPH	$C_{10}H_{10}N_4O_4$	249.0624	4.5
MVK	C_4H_6O	70.0419	MVK-DNPH	$C_{10}H_{10}N_4O_4$	249.0624	4.8
Benzaldehyde	C_7H_6O	106.0419	Benzaldehyde-DNPH	$C_{13}H_{10}N_4O_4$	285.0624	5.4
Glyoxal	$C_2H_2O_2$	58.0055	Glyoxal-bis-DNPH	$C_{14}H_{10}N_8O_8$	417.0534	5.7
Norcamphor	$C_7H_{10}O$	110.0732	Norcamphor-DNPH	$C_{13}H_{14}N_4O_4$	289.0937	5.7
Methylglyoxal	$C_3H_4O_2$	72.0211	Methylglyoxal-bis-DNPH	$C_{15}H_{12}N_8O_8$	431.0700	6.5
Diacetyl	$C_4H_6O_2$	86.0368	Diacetyl-bis-DNPH	$C_{16}H_{14}N_8O_8$	445.0856	7.2
Nopinone	$C_9H_{14}O$	138.1045	Nopinone-DNPH	$C_{15}H_{18}N_4O_4$	317.1250	7.8
Camphor	$C_{10}H_{16}O$	152.1201	Camphor-DNPH	$C_{16}H_{20}N_4O_4$	331.1412	8.2

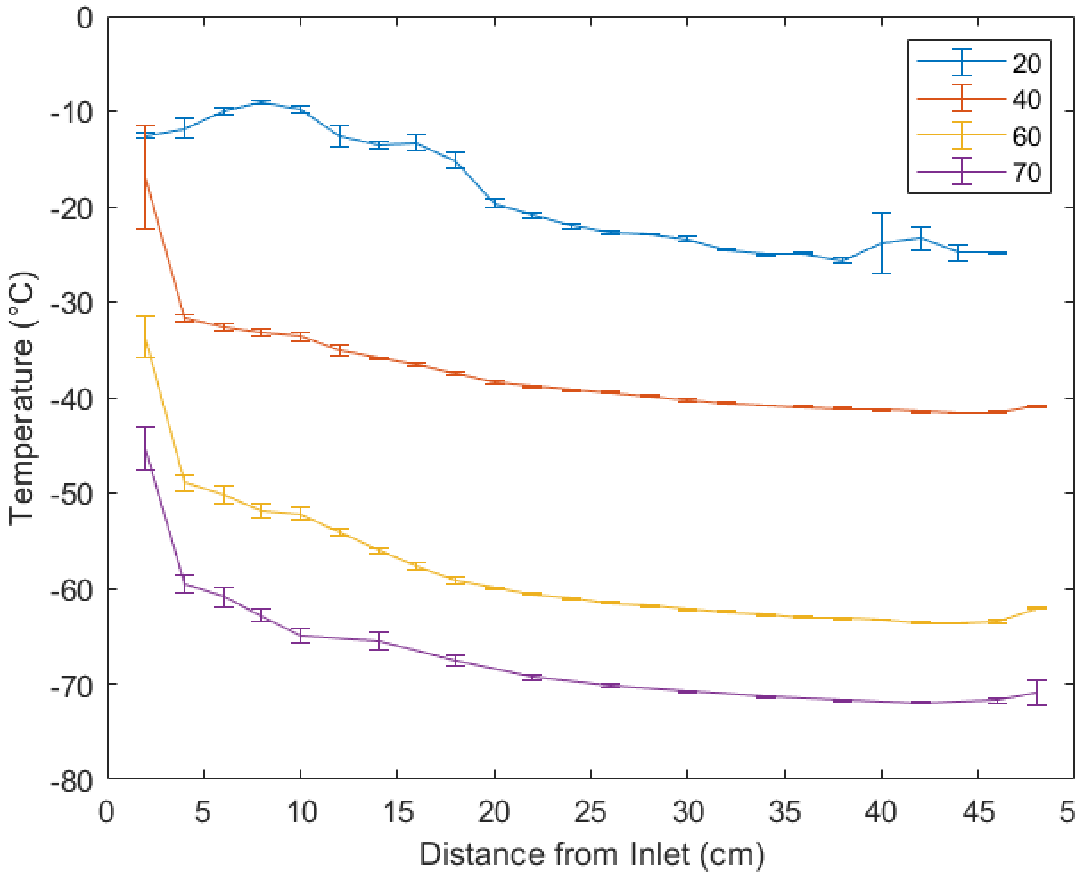

Figure S1. Temperature Profile along z-axis of Flowtube

Section S1. Discussion on Entropy-Enthalpy Compensation

Reviewing this data in accordance with the definitions laid out by Liu and Guo, (2001) and Pan et al. (2015), it appears unlikely that the Entropy-Enthalpy Compensation (EEC) effect seen here is a spurious finding. The linearity from the regressions in Table 3 are strong and thus there is relatively low standard error in ΔH and ΔS, especially comparing to the significant range of ΔH and ΔS values (–145 to 21 kJ mol^{-1}, –621 to 44 J mol^{-1} K^{-1} respectively). The lack of strong convergence to an isoequilibrium when extrapolating from Figure 2 (also more clearly demonstrated in Figure S2) shows that this system however does not readily appear to meet the definitions to be an isokinetic relation (IKR).

This correlation between ΔS and ΔH can further be explored under the constraints that Sharp (2001) places on EEC for 95% confidence. The range of ΔG in this experiment is from –9 to 24.4 kJ mol^{-1} while the range of temperatures experiments were run was between –20 and –40 °C, (the harmonic mean being –30.3 °C or 242.9 K). While $|\Delta G| < |\Delta H|$ for most cases here, there is a significant range of $|\Delta G|$ and in the same magnitude as $|\Delta H|$ such that ΔG cannot be considered constant. The compensation temperature (235.5 K) however does fall within the 2σ range of the experimental temperature (242.9 K) and so this analysis alone does not meet the 95% confidence interval for nontrivial correlation. But, if the data from Fries et al. (2007) is included in this analysis, Tc and r^2 are instead 225.9 K and 0.9788 respectively with the harmonic mean experimental temperature as 244.9 K; this places Tc outside of the 2σ range of the experimental temperature and thus meets Sharp's criteria for a nontrivial correlation.

In regards to IKR as viewed through the Griessen et al. (2020) and Griessen and Dam (2021) EEC analysis, the Compensation Quality Factor (CQF) values are rather low, both below 0.25. This supports the observation of the absence of strong coalescence to an isoequilbrium and no noticeable IKR. The increase in CQF when including the data from Fries et al. (2007) also indicates that with the inclusion of more data, coalescence could be statistically inferred.

It should be noted that the explanation of EEC from solvation effects is not specific to aqueous systems. Computational work has identified instead two causes for EEC in solvent-solute interactions: solvent reorganization and molar shift (Grunwald and Steel, 1995). Regardless of aqueous nonspecificity, the EEC's implication of a surface liquid layer can still be made. There are other less likely potential explanations currently in literature such as the influence of hidden Carnot cycles from microphase transitions (Starikov and Nordén, 2007) or the loss of translational and rotational entropy during gas phase association (Ryde, 2014). However, these seem unlikely to be the dominant mechanism for the EEC seen here and are outside the scope of discussion here.

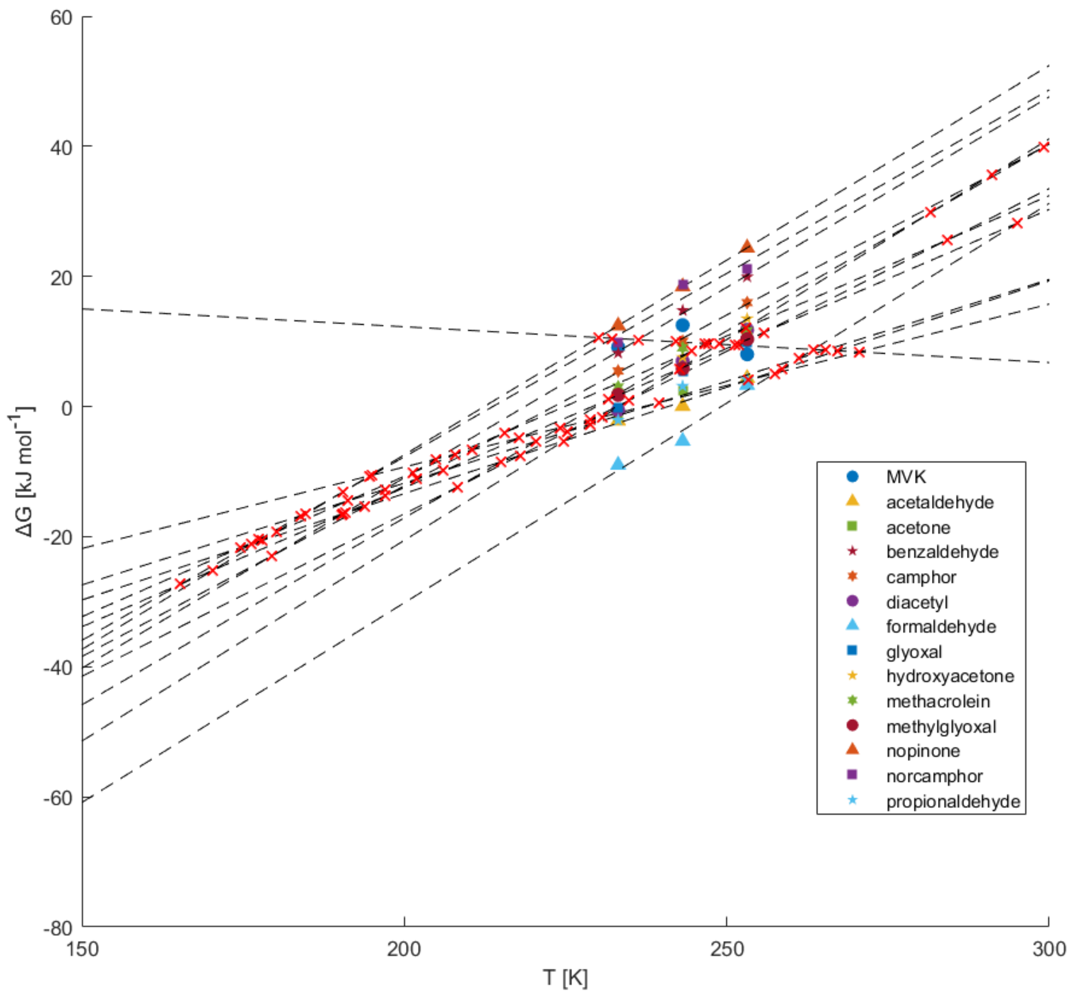

Figure S2. Plot of Temperature versus ΔG. Red x's indicate intersections of the extrapolated linear regressions.

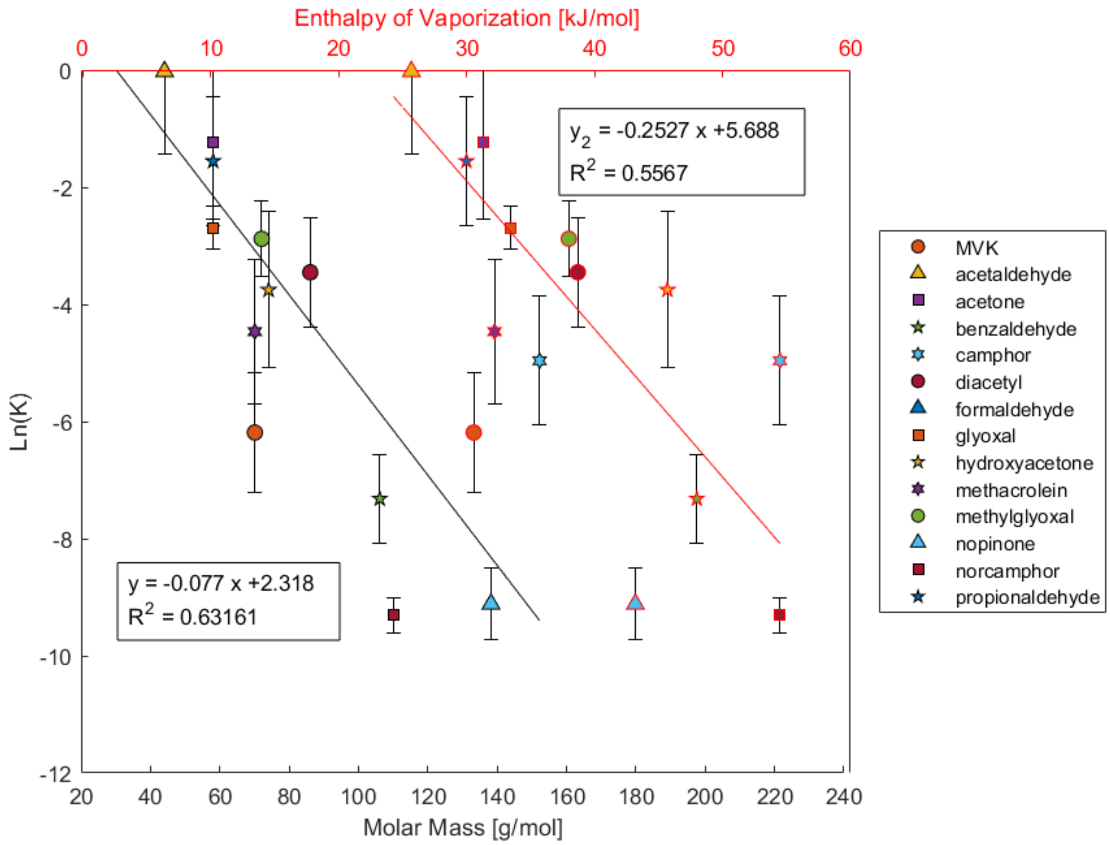

Figure S3. Scatterplot of ln(K) at –30 ºC versus the heat of vaporization (red line) and molar mass (black line).

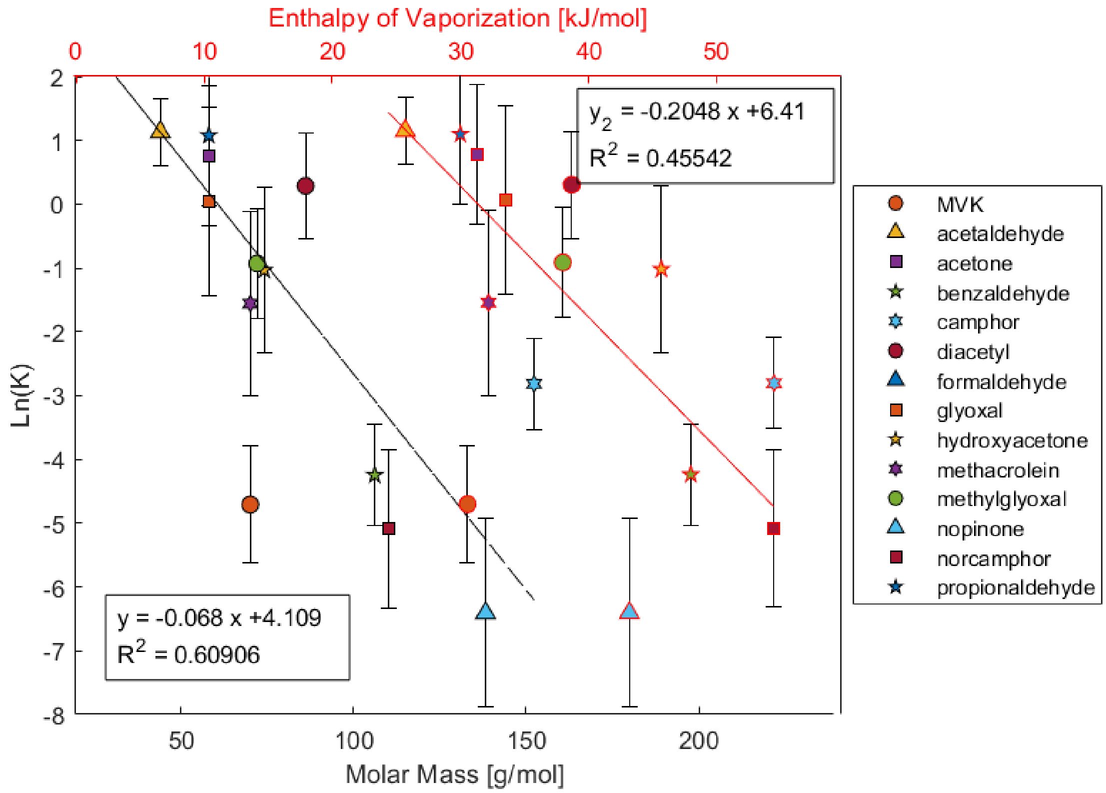

Figure S4. Scatterplot of ln(K) at –40 ºC versus the heat of vaporization (red line) and molar mass (black line).

References

Fries, E., Starokozhev, E., Haunold, W., Jaeschke, W., Mitra, S. K., Borrmann, S., and Schmidt, M. U.: Laboratory studies on the uptake of aromatic hydrocarbons by ice crystals during vapor depositional crystal growth, Atmos Environ, 41, 6156–6166, https://doi.org/10.1016/j.atmosenv.2007.04.028, 2007.

Griessen, R. and Dam, B.: Simple Accurate Verification of Enthalpy-Entropy Compensation and Isoequilibrium Relationship, ChemPhysChem, 22, 1774–1784, https://doi.org/10.1002/CPHC.202100431, 2021.

Griessen, R., Boelsma, C., Schreuders, H., Broedersz, C. P., Gremaud, R., and Dam, B.: Single Quality Factor for Enthalpy-Entropy Compensation, Isoequilibrium and Isokinetic Relationships, ChemPhysChem, 21, 1632–1643, https://doi.org/10.1002/CPHC.202000390, 2020.

Grunwald, E. and Steel, C.: Solvent Reorganization and Thermodynamic Enthalpy-Entropy Compensation, J. Am. Chem. Soc, 5687–5692 pp., 1995.

Liu, L. and Guo, Q. X.: Isokinetic relationship, isoequilibrium relationship, and enthalpy-entropy compensation, https://doi.org/10.1021/cr990416z, March 2001.

Pan, A., Biswas, T., Rakshit, A. K., and Moulik, S. P.: Enthalpy-Entropy Compensation (EEC) Effect: A Revisit, Journal of Physical Chemistry B, 119, 15876–15884, https://doi.org/10.1021/acs.jpcb.5b09925, 2015.

Ryde, U.: A fundamental view of enthalpy-entropy compensation, Medchemcomm, 5, 1324–1336, https://doi.org/10.1039/c4md00057a, 2014.

Sharp, K.: Entropy—enthalpy compensation: Fact or artifact?, Protein Science, 10, 661–667, https://doi.org/10.1110/ps.37801, 2001.

Starikov, E. B. and Nordén, B.: Enthalpy-entropy compensation: A phantom or something useful?, Journal of Physical Chemistry B, 111, 14431–14435, https://doi.org/10.1021/JP075784I/ASSET/IMAGES/LARGE/JP075784IF00001.JPEG, 2007.